Pharmaceutical Research, Vol. 23, No. 7, July 2006 (© 2006)
DOI: 10.1007/s11095-006-0256-z

Research Paper

A Novel Tool to Characterize Paracellular Transport: The APTS–Dextran Ladder

Winfried Neuhaus,[1] Elisabeth Bogner,[2] Michael Wirth,[2] Joanna Trzeciak,[1] Bodo Lachmann,[1] Franz Gabor,[2] and Christian R. Noe[1,3]

Received January 1, 2006; accepted February 17, 2006

Purpose. The aim of this work was to develop an easy, manageable, and precise analytic tool to describe the tightness of cell layers by a molecular weight ladder.
Methods. Dextrans were labeled by reductive amination with fluorescent 8-aminopyrene-1,3,6-trisulfonate (APTS). This mixture, including the internal standard diazepam, was used for transport studies in Transwell models using Caco-2, ECV304, and PBMEC/C1–2 cell lines. Samples were analyzed by fluorimetry, capillary electrophoresis, and reverse-phase high-performance liquid chromatography.
Results. Following this approach, a logarithm correlation of R^2 = 0.8958 between transepithelial electrical resistance (TEER) and APTS–dextran permeability was shown. In addition, a TEER-dependent permeability pattern could be observed including each single fraction from free APTS, APTS–glucose up to APTS–dextran consisting of 35 glucose units. The TEER-independent permeability coefficients of diazepam and confocal laser scanning microscopy images confirmed the paracellular transport of APTS–dextran.
Conclusions. All in all, the developed APTS–dextran ladder is a useful tool to characterize cell layer tightness and especially to describe paracellular transport ways and the extent of leakiness of cell layers (for blood–brain barrier or intestinal studies) over time—applying a wide array from smaller to larger molecules at the same time to refine TEER, sucrose, or Evans blue measurements.

KEY WORDS: APTS–dextran; BBB; blood–brain barrier; cell layer tightness; paracellular transport.

INTRODUCTION

The development of new drugs determining a directed transport across epithelial and endothelial barriers is one of the major tasks in pharmaceutical sciences. In the past few decades, research has mainly focused on search for novel drug targets and design of novel drugs rather than on drug delivery (1). Particularly, the drug delivery of poorly available drugs is often problematic. This indicates the need to improve the permeation ability of drugs through the various biological barriers by taking into consideration the particular transport mechanisms.

In this regard, it is also essential to learn more about the correlation between tightness status of membranes and permeation of drugs. Tightness of cell layers is mainly characterized by the building of tight junctions, but development is not initiated until a confluent cell layer has been formed (2). Bands of tight junctions (zonula occludens) between adjacent cells restrict the paracellular pathway and effectively prevent the passage of polar, hydrophilic drugs between cells, whereas in non-barrier-forming epithelia or endothelia, the bands contain focal discontinuities. The resulting distinct tightness of membrane junctions is reflected in a high transmembrane electrical resistance. Limiting factors concerning drug transport, therefore, are the lipophilic qualities and size of the respective molecules, which results either in a paracellular or a transcellular transport mechanism. The paracellular transport is important for small hydrophilic molecules and happens mainly through the tight junctions, whereas during transcellular transport, lipophilic molecules have to permeate directly the lipid bilayer of the cells (3). The characterization of the paracellular transport route has been investigated with various substances. Especially, determination of the permeability of sucrose, Evans blue, or fluorescein isothiocyanate (FITC)-labeled dextrans

[1] Department of Medicinal Chemistry, University of Vienna, Pharmacy Center, Althanstrasse 14, A-1090 Vienna, Austria.
[2] Department of Pharmaceutical Technology and Biopharmaceutics, University of Vienna, Pharmacy Center, Althanstrasse 14, A-1090 Vienna, Austria.
[3] To whom correspondence should be addressed. (e-mail: christian.noe@univie.ac.at)

ABBREVIATIONS: ACM, astrocyte conditioned medium; APTS, 8-aminopyrene-1,3,6-trisulfonate; BBB, blood–brain barrier; BMECs, brain microvascular endothelial cells; CLSM, confocal laser scanning microscopy; FD, FITC dextran; FITC, fluorescein isothiocyanate; LIF detector, laser-induced fluorescence detector; P-gP, P-glycoprotein; TEER, transendothelial electrical resistance for studies with cell lines ECV304 and PBMEC/C1–2, transepithelial electrical resistance in case of Caco-2; vWF, von Willebrand factor; γ-GT, γ-glutamyltransferase.

(FDs) have become methods of choice to elucidate the tightness status *in vivo* or *in vitro* next to transendothelial or transepithelial electrical resistance (TEER). At least since the late 1980s, it has been known that commercially available FDs contain varying amounts of free FITC (4) and consist of a wide range of polymers with different molecular weights. Commonly, total fluorescence values have been measured in permeation studies without considering the size of the different fluorescent fractions. If leakiness of the barrier membrane occurs—for instance, due to lack of fully functional tight junctions—the TEER decreases, whereas the permeability of sucrose, Evans blue, and FDs should increase. In this context, the relationship between molecular weight and permeability through a cell layer at a distinct tightness status is not well described. Several studies for comprehensive tightness characterization were carried out using different types of molecules with different molecular weights (5–8), but still no method to measure a permeability pattern based on molecular weights of similar oligomeric molecules exists. Obviously, dextran, a glucose polymer, seems to possess an adequate structure for the design of such a molecular size ladder. Due to its multifunctionality, labeling can be easily achieved either at the hydroxyl or at the carbonyl group. Furthermore, it is cheap and easy to obtain.

To prove the potential applicability of the presented 8-aminopyrene-1,3,6-trisulfonate (APTS)–dextran ladder for tightness characterization, three different cell culture models were selected. Caco-2 cells represent a well-established model for the human intestinal epithelium and, thus, for estimation of the availability of oral drugs, although they originate from a human colon adenocarcinoma. Upon reaching confluency, the cells spontaneously differentiate to an intestinal phenotype. This differentiation is indicated morphologically by the appearance of microvilli, and functionally by the activity of a set of brush border enzymes at the apical membrane (2,9). To date, the Caco-2 model is approved by the FDA to determine drug permeability *in vitro* in terms of the biopharmaceutical classification system and bioequivalence studies (10–12).

Moreover, Caco-2 monolayers are characterized by the formation of tight junctions that seal the apical membrane, resulting in a distinct transepithelial electrical resistance upon growth on filters (13,14). Because of its striking similarities to the human intestinal epithelium and broad acceptance as well as high TEER values, the Caco-2 cell line seems to be most appropriate for these studies.

Additionally, due to the importance of paracellular tightness for the blood–brain barrier (BBB), two BBB-mimicking cell lines were used for these studies. The BBB maintains the homeostasis of the brain microenvironment, which is crucial for neuronal activity and function. Brain microvascular endothelial cells (BMECs) that constitute the BBB are responsible for the transport of nutrients to neurons and clearance of potentially toxic substances from the brain. Unlike the peripheral endothelium, BMECs are characterized by the presence of tight intercellular junctions, minimal pinocytotic activity, and the absence of fenestrations (15). Typically, electrical resistance values of about 2000 Ω cm^2 are observed in pial microvessels on the surface of the brain (16) as compared to 1–3 Ω cm^2 in mesenteric capillaries (17) *in vivo*.

The ECV304 cell line, which was introduced by Takahashi *et al.* (18), exhibits increased TEER when cocultured with rat C6 glioma cells (19,20) or grown in astrocyte conditioned medium (ACM). This increase mimics the development of BBB features when peripheral endothelial cells are cultured with astrocytes (21). Furthermore, upregulation of the glucose transporter GLUT1 and of gamma glutamyl transpeptidase in astrocyte-cocultured ECV304 were reported (22). In addition, ECV304 developed other BBB characteristics including transferrin receptor expression and P-glycoprotein (P-gP) when cocultured with C6 (23). As a second BBB model, the cell line PBMEC/C1–2 was included in the investigations. In earlier studies of our research, group effects of glioma C6 rat cell line conditioned medium on TEER and permeability in a Transwell model with PBMEC/C1–2 were described (24). Typical endothelial markers like von Willebrand factor (vWF) and apolipoprotein A-1 as well as BBB markers like γ-glutamyltransferase (γ-GT) and glucose transporter GLUT-1 were detected in immortalized PBMEC/C1–2 (25). Furthermore, no difference was found in PBMEC/C1–2 in passages 91 to 198 investigating LDL uptake, expression of vWF, expression of P-gP and activity of γ-GT (26). Moreover, PBMEC/C1–2 was used to investigate the invasion of porcine BMEC by *Streptococcus suis* serotype 2 (27) and by *Haemophilus parasuis* (28).

The aim of this study was to develop and evaluate a novel method to characterize the tightness status of cell layers. The correlation of TEER with the total permeability of APTS–dextran was assessed, and it was investigated whether molecular-weight-dependent permeability patterns of APTS-labeled dextran are TEER dependent. Transport studies with diazepam, a benzodiazepine that is supposed to permeate by passive diffusion, at different TEER, and confocal laser scanning microscopy (CLSM) were carried out to verify the paracellular transport of the APTS-labeled dextran.

MATERIALS AND METHODS

Materials

RPMI 1640, Dulbecco's modified Eagle's medium (DMEM), amphotericin B, transferrin, APTS, and gelatin were purchased from Sigma (St. Louis, MO, USA). L-Glutamine for Caco-2 was obtained from Merck (Darmstadt, Germany). Gentamicin sulfate and fetal calf serum (FCS) were from Biochrom AG (Berlin, Germany).

Iscove's modified Dulbecco's medium (IMDM), Ham's F-12, NCS, L-glutamine, penicillin/streptomycin, and nonessential amino acids were obtained from Invitrogen Life Technologies (Gibco™, Carlsbad, CA, USA). Heparin was purchased from MP Biomedicals (Irvine, CA, USA). Dextran (average MW = 6000) was from Fluka (Buchs, Switzerland). Collagen was purchased from ICN Biomedicals Inc. (Aurora, OH, USA). Fibronectin was obtained from BD Biosciences (Bedford, MA, USA) as well as Transwell inserts (Falcon™, Bedford, MA, USA) and six-well plates (Falcon™).

Diazepam was a kind gift from Dr. Maierhofer (Bundesanstalt für chemische und pharmazeutische Untersuchungen, Vienna, Austria). Inorganic salts and all other reagents were of analytical grade.

Cell Culture

The Caco-2 cell line was obtained from the American Type Culture Collection (Rockville, MD, USA). Cells maintained in RPMI 1640 medium were used at passage 48, whereas cells maintained in DMEM were used at passages between 23 and 48. Caco-2 cells were cultured in media containing 10% FCS, 4 mM L-glutamine, 150 μg/mL gentamicin, and in case of DMEM, additional 1% nonessential amino acids.

PBMEC/C1–2 were established and characterized by Teifel and Friedel (25) and were a kind gift from them. C6 cells derived from rat glioma (29) were obtained from the German Cancer Research Center Heidelberg (DKFZ, Heidelberg, Germany). C6 cells were grown at passages 23 to 50 in 175 cm^2 gelatin-coated tissue flasks (Greiner Bio-One GmbH, Frickenhausen, Germany) in C6 medium, which consists of IF medium (1:1 mixture of IMDM and Ham's F-12), supplemented with 7.5% (v/v) NCS, 7 mM L-glutamine, 5 μg/mL transferrin, 0.5 U/mL heparin, 100 U/mL penicillin, 100 μg/mL streptomycin, and 0.25 μg/mL amphotericin B. To obtain ACM, the supernatant of C6 cultures was collected every other day. PBMEC/C1–2 were grown in 25 cm^2 gelatin-coated tissue culture flasks in PBMEC medium (50% C6 medium, 50% ACM) at passages 55–67. Before use, PBMEC medium was sterile filtered additionally as already described in detail (24).

The ECV304 cell line was obtained from the European Collection of Cell Cultures (ECACC, Wiltshire, UK). Cells at passages 145–149 were maintained in PBMEC medium as described above.

All cells were cultured in a humidified 5% CO_2/96% humidity at 37°C and subcultivated by trypsination every 3 to 4 days.

Labeling Reaction

To develop a system that enables discrimination between several molecular weight fractions, dextrans (average MW = 5779 g/mol, MW/MN = 2.39) were labeled with APTS by reductive amination and analyzed by capillary electrophoresis (CE). The labeling reaction (Fig. 1) was performed as reported (30–32) with slight modifications. In brief, the dextran solution was not dried, it was dissolved in a total volume of 20 μL bidest. H_2O. The $NaBH_3CN$ was dissolved in MeOH instead of THF. The labeling mixture consisting of 20 μL dextran, 5 μL 0.1 M APTS (in 1 M citric acid), and 7.5 μL 1 M $NaBH_3CN$ was incubated at 85°C for 3.5 h.

Fluorescence Measurements

The total fluorescence of APTS-labeled dextran was determined by using a microplate reader (polarstar galaxy, BMG Labtech, Offenburg, Germany) at an excitation wave length of 485 nm and an emission filter at 520 nm.

Capillary Electrophoresis

All separations were performed at 25°C using a P/ACE 5500 system with a laser-induced fluorescence (LIF) detector (Beckman Instruments), Ar laser (excitation at 488 nm, emission wavelength of 520 nm), and System Gold 8.0 software. The detector was situated 7 cm from the anodic end (reverse polarity); injection by pressure was accomplished with 3.45 kPa for 4.0 s.

For FITC–dextran analysis, deactivated fused silica capillary columns (Ziemer Chromatographie, Mannheim, Germany; methyl/silyl derivatized, 100 μm I.D., 360 μm O.D., 37 cm length) and a TBE buffer solution consisting of 44.5 mM Tris, 44.5 mM boric acid, 2 mM EDTA, and 0.5% hydroxypropylmethylcellulose (HPMC) were used at 20 kV.

To separate APTS–dextran, neutral capillary columns (50 μm I.D., 47 cm length, Beckman Coulter, Fullerton, CA, USA) were used and a buffer solution consisting of 25 mM LiAc (pH 4.75) and 0.4% PEO (MW = 8,000,000) was applied at 23.5 kV. Before every run, the capillary was flushed for 1 min with water and then 4 min with separation buffer. After derivatization, the fraction pattern was checked prior to first application for transport studies. Validation data were reported (33).

Reverse-Phase High-Performance Liquid Chromatography of Diazepam

For the analysis of diazepam, reverse-phase high-performance liquid chromatography (RP-HPLC) was used (La Chrom L-7100 pump, autosampler L-7200, UV–VIS detector L-4250, Merck-Hitachi, VWR International Inc., West Chester, PA, USA; column: Lichrospher 100 RP-18, 250 × 4 mm, 5 μm pore size, Merck KGaA, Darmstadt, Germany; 25°C operating temperature by column thermostat BFO-04, W.O. Electronics, Langenzersdorf, Austria). A mixture of methanol, acetonitrile, and water (20:45:35) was used as mobile phase. Samples were precipitated with methanol before analysis.

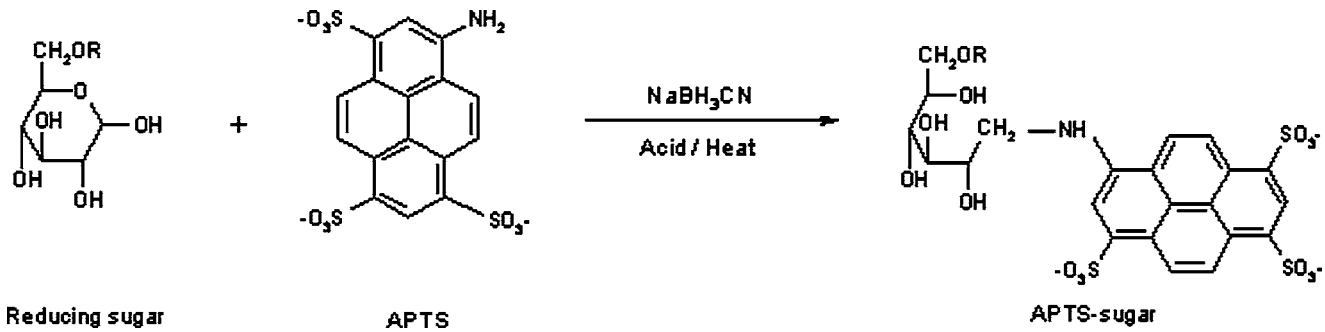

Fig. 1. Scheme of the labeling reaction, a reductive amination of reducing sugars with APTS.

Transport Studies

The inserts were coated with collagen and fibronectin for Caco-2 and PBMEC/C1–2 and with collagen only for ECV304 cells. For permeation experiments the cells were seeded at a density of $2.86 \times 10^4/cm^2$ (Caco-2) or 8×10^4 cells/cm^2 (PBMEC/C1–2 and ECV304) and grown to confluency on membrane filter inserts. The culture medium was changed every other day up to the transport studies. For PBMEC/C1–2, the medium was especially supplemented with 1 μg/mL fibronectin for enhanced attachment. Cell monolayers of Caco-2 in DMEM were used for transport studies for 5–28 days, Caco-2 in RPMI medium for 5–7 days, PBMEC/C1–2 for 3–5 days, and ECV304 for 10–14 days after seeding.

The TEER was measured daily with a Millipore Millicell Electrical Resistance System (ERS, Millipore, Vienna, Austria) after changing the medium. Control measurements from blank inserts were subtracted to calculate the TEER of the cell layer. Resistance values were multiplied by the surface area of the insert (4.2 cm^2) and expressed in ohms centimeter squared.

After visual control of cell monolayers using light microscopy and determination of the TEER, transport studies with APTS–dextran 6000 (240 μM in culturing medium) were accomplished. APTS-labeled dextran was used to characterize the paracellular transport route. To describe transcellular transport as well, diazepam was used as an internal standard. Diazepam is supposed to permeate by passive diffusion (34–36) and was added at concentrations of 50 μM to APTS–dextran test solutions.

Each well was equilibrated with 3 mL DMEM or RPMI medium for Caco-2 and C6 medium for PBMEC/C1–2 and ECV304 for 30 min at 37°C. For blank values, the coated filter inserts were incubated in medium for at least 45 min to ensure sufficient swelling. Inserts were placed into prepared wells and the donor chamber was loaded with the analyte solution. Each filter insert was transferred at several time points into the next well containing 3 mL medium to maintain sink conditions. Additionally, saturation kinetics of the transport could be followed as a control. The transferring intervals for APTS–dextran studies were dependent on the TEER of the investigated cell monolayer. At the end of transport studies, the supernatant of the inserts was removed and analyzed to estimate substance recovery rates. Inserts were transferred into wells with fresh medium and the apical chamber was refilled with medium. After temperature equilibrium was reached, TEER was determined to prove that there was no occurrence of adverse effects on tight junction function due to test solution application.

Total fluorescence of APTS–dextrans of the individual samples was determined using a microplate reader, followed by CE as described above. Thus, percentages of total fluorescence of every single peak were determined and clearance values were calculated according to Eq. (1) for cultured membrane inserts and blank values.

$$clearance = \frac{C_{B_n} V_B}{C_A - (V_B/V_A \times \sum C_{B_{n-1}})} \quad (1)$$

C_{Bn} refers to the substance concentration in the basolateral chamber, C_A is the concentration in the apical compartment, and V_A and V_B are the corresponding volumes of the chambers. Because the amount of the test compound in the apical insert decreases over time under conditions of unidirectional flux, the C_A value for each time point (each well) has to be corrected. Thus, the summed-up total amount of substance found in each basolateral compartment before the actual one ($\sum C_{Bn-1}$) is related to the apical volume and subtracted from C_A. For calculating permeability coefficients, slope of clearance *vs.* time is determined by linear regression analysis and multiplied with a factor considering the growth surface area (4.2 cm^2). Finally, results of blank value experiments were included into permeability coefficient calculation by using reciprocal correlation, shown in Eq. (2). PE_{blank} refers to the permeability coefficient without cell layer, PE_{all} represents the permeability coefficient through membrane insert and the cell layer, and PE_{cell} is the permeability coefficient through only the cell layer.

$$\frac{1}{PE_{cell}} = \frac{1}{PE_{all}} - \frac{1}{PE_{blank}} \quad (2)$$

Diazepam was analyzed by RP-HPLC. Permeability coefficients were determined by the same procedure as described above.

Confocal Laser Scanning Microscopy

CLSM of the monolayers was performed immediately after the transport study. After removal of the transport medium, the layer was washed once with 500 μL PBS. Then, the filter membrane was detached and mounted for CLSM using FluorSave Reagent.

Confocal images of fluorescent dextran located in-between the cells were obtained using a Zeiss Axiovert confocal microscope (LSM 410 invert, Zeiss, Jena, Germany). Pictures were acquired at a magnification of 63× and the black level of the green fluorescence detector was adjusted to eliminate any autofluorescence of unstained cells. APTS–dextran was detected by excitation at 488 nm and emission at 510–525 nm.

To estimate cellular viability, additional monolayers were incubated with 500 μL of a solution containing 2 μg propidium iodide/mL PBS for 15 min at RT after removal of excess APTS–dextran. Then, the cell layers were washed, mounted for microscopy, and analyzed by CLSM, as described above, at 488/510–525 nm and at 488/>590 nm.

RESULTS

The APTS–dextran ladder was developed as a new tool to characterize paracellular transport. The dextran solution contains a wide range of oligomers with different sizes. Apart from the measurement of total fluorescence intensities with a microplate reader, the APTS labeling of dextran offers also the possibility to determine the single fractions by CE simultaneously and individually.

Capillary Electrophoresis

Figure 2A demonstrates a typical electropherogram of commercially available FD4 (Sigma) in C6 medium with a single peak of FITC and a broad hill of FD4 representing the

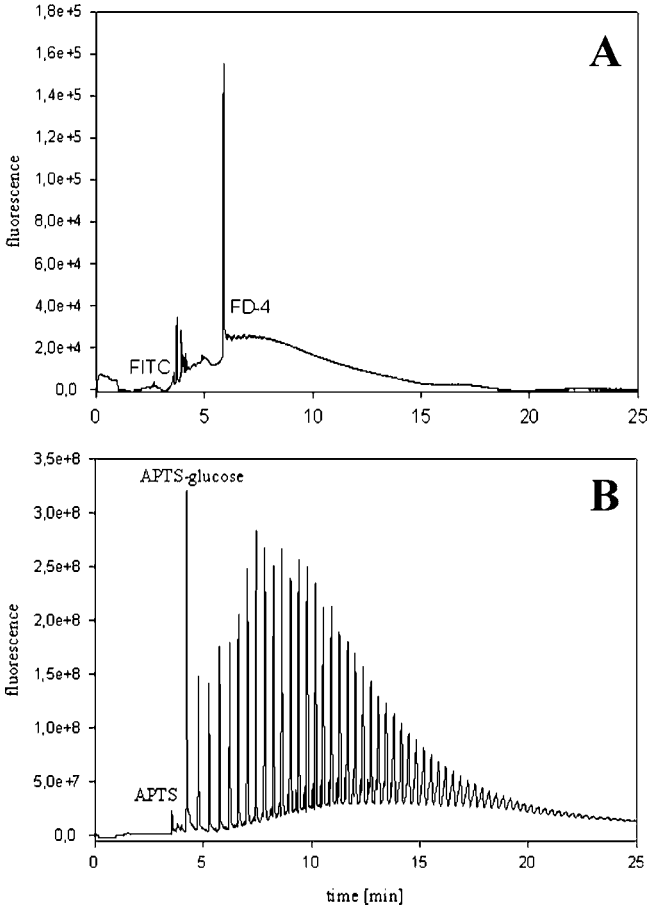

Fig. 2. (A) Typical electropherogram of FD4 in C6 medium. It is not able to differentiate between several fractions besides the early FITC peak. (B) Electropherogram of APTS-labeled dextran 6000 in C6 medium. In comparison to FD4, every single peak of APTS–dextran 6000 is analyzable. The molecular weight of each fraction is increased by about one glucose unit compared to its left neighboring peak.

distribution of an unseparated mixture of dextrans. Electropherograms of FDs only allow correction of permeability coefficients regarding the free amount of FITC. Further work concentrated on the separation of mixtures of several purchasable FDs with different average molecular weights (FD4, FD10S, FD20, and FD40, Sigma). However, this approach did not lead to effective results because no sufficient resolution between these mixtures of FDs were achieved by CE. Additionally, in-house labeling of dextrans with FITC was also not successful because FITC binds to hydroxyl groups of dextran in a statistical manner, and thus separation was not possible due to the variable mass/charge relations of FITC-labeled dextrans. For exact measurements, a molecular ratio of 1:1 between dextran and fluorescent marker is necessary. Based on previous experience (37–39), a terminal carbonyl moiety reacts easily in reductive amination. Because of its comparable fluorescent properties to FITC, APTS was chosen and covalently linked to dextran molecules. Figure 2B shows an electropherogram of APTS-labeled dextran 6000. Due to the specific reductive amination, separation was remarkably improved. After labeling, each dextran fraction is linked to one APTS molecule giving all products the same charge. Consequently, using PEO as polymeric additive migration through the electrical field was only dependent on molecular size and weight. Thus, every single fraction of the APTS–dextran could be determined separately due to an improved CE method and this change of labeling strategy.

Transport Studies

Correlation of TEER and Total APTS–Dextran Permeability

To correlate the TEER with the permeability of fluorescent APTS-labeled dextran 6000 across monolayers with different TEER values, transport studies with Caco-2 cell monolayers cultured in DMEM were performed. Total fluorescence intensities of APTS-labeled dextran 6000 (in DMEM) solutions in the apical and basolateral compartment were analyzed followed by calculation of permeability coefficients. In the case of paracellular transport, less permeability at increased TEER is expected. Hence, the inserts were transferred at several time points, dependent on the TEER value of the used cell monolayer, to gain detectable fluorescent signals. For example, inserts with a TEER of 0–60 Ω cm^2 were transferred every 20 min, whereas inserts with 60–120 Ω cm^2 were transferred every 45 min, 121–160 Ω cm^2 every 60 up to 240 min, 161–180 Ω cm^2 every 380 min, 181–320 Ω cm^2 every 18 h, 321–420 Ω cm^2 every 44 h, and inserts with up to approximately 510 Ω cm^2 every 74 h. The presented PE data originated from first samples to minimize influence of possibly increased TEER during the experiment and therefore assure highest comparability between obtained permeability coefficients at different TEER values. However, linearity of clearance *vs.* time curves were granted for transport studies with more samples (data not shown).

Correlation between TEER and APTS–dextran permeability is shown in Fig. 3. In the figure, every data point represents a single cultured Transwell insert with specific TEER. Curve progression (Fig. 3A) suggested an exponential correlation between TEER and APTS–dextran permeability. Thus, log PE_{cell} was calculated and depicted in relation to the appropriate TEER in Fig. 3B. Linear regression analysis resulted in a correlation coefficient R^2 of 0.8958, which confirmed the exponential correlation between TEER of Caco-2 cells cultured in DMEM and APTS–dextran permeability. Additionally, transport studies with monolayers of Caco-2 cells cultured in RPMI medium as well as with ECV304 and PBMEC/C1–2 were carried out at different TEER to assess this correlation also for these monolayers. The results are shown in Fig. 3A and B. The observed correlation between TEER and APTS–dextran permeability was in a similar range like those of Caco-2 cells in DMEM with some minor differences. For example, the permeability through PBMEC/C1–2 monolayers was about 9.49 ± 0.12 μm/min at TEER of 100 ± 8 Ω cm^2 (n = 3) in comparison to ECV304 with 1.85 ± 0.18 μm/min at TEER of 122 ± 15 Ω cm^2 (n = 3). After transport experiments TEER measurements of both cell monolayers in apical APTS– dextran solution as well as after supernatant removal and temperature equilibrium in growth medium indicated no breakdown of tight junctions. Recovery rates of APTS– dextran were about 100% for blank experiments and 85–97% for cell experiments.

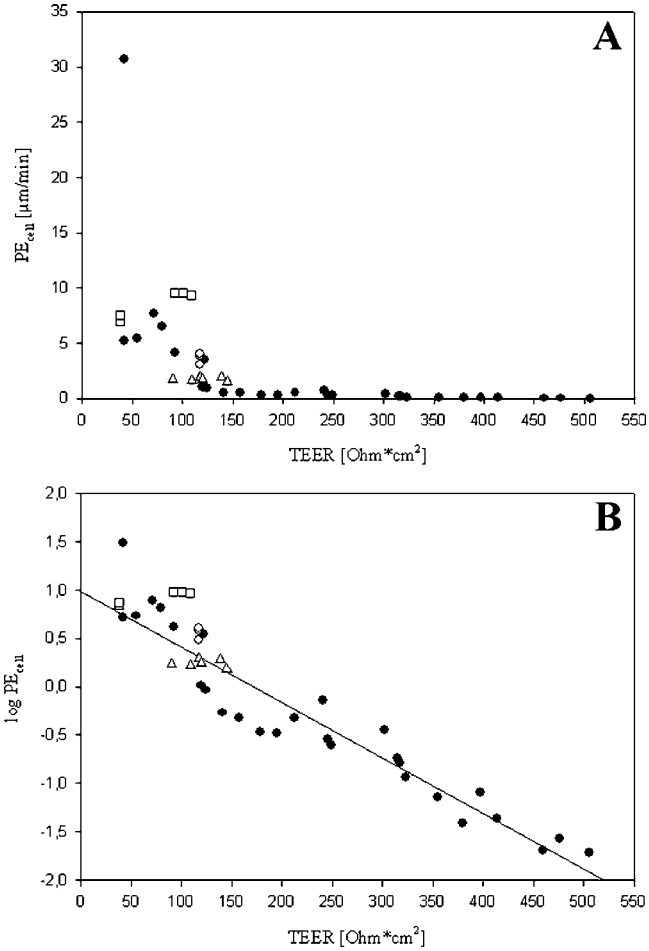

Fig. 3. Summary of transport studies with APTS–dextran 6000. Correlation between TEER and total permeability coefficients PE_{cell} (A) or log PE_{cell} (B) of transport studies across Caco-2 cell monolayers cultured in DMEM (•), in RPMI (○), and across ECV304 (△) and PBMEC/C1–2 (□) cell monolayers.

TEER-Dependent APTS–Dextran Permeability Pattern

A main advantage of APTS–dextran for characterization of cell layer tightness is the possibility of determination of a size-dependent permeability pattern. Capillary electrophoresis was used to obtain fluorescence values for every single fraction of the applied APTS–dextran mixture followed by calculation of respective permeability coefficients. Every single fraction in the electropherogram just differs about one glucose unit from the neighbored one. Therefore, it is possible to obtain a permeability pattern for a distinct tightness status with a high resolution between the data points of about one glucose unit. For better comparability of the changes of permeability pattern at different TEER values, permeability coefficients of every single fraction were related to the permeability of APTS, which was set to 100%. Figure 4 summarizes these results at different TEER values of Caco-2 monolayers cultured in DMEM. No significant difference in permeability was detected between APTS and APTS–dextran with 35 glucose units at 42 Ω cm^2. Increase of TEER led to a change of the permeability pattern. Linear regression analysis was applied for the individual curves. At a TEER of 42 Ω cm^2 the slope of the curve was 0.06

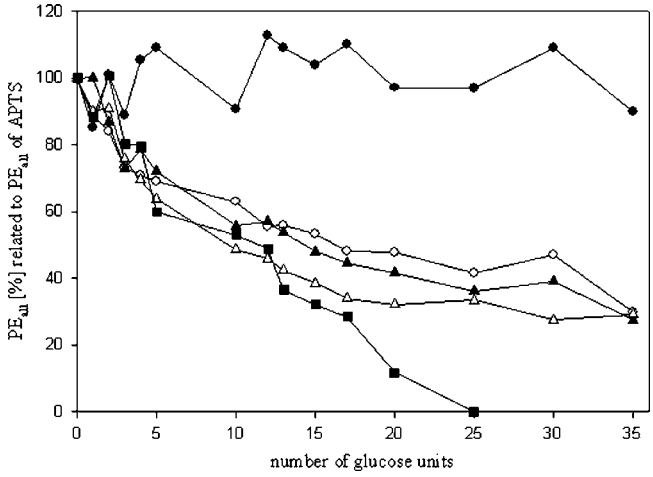

Fig. 4. TEER-dependent permeability pattern of APTS–dextran 6000. Permeability coefficients were related to the fluorescent APTS (glucose number = 0) at a TEER of 42 (•), 124 (○), 179 (▲), 317 (△), and 460 (■) Ω cm^2.

and decreased continuously to −1.60 at 124 Ω cm^2, to −1.94 at 179 Ω cm^2, to −2.01 at 317 Ω cm^2, and finally to −3.60 at 460 Ω cm^2.

To illustrate the significant changes in permeability patterns at different TEER, the permeability values of the individual APTS–dextran fractions with specific molecular weight were calculated for Caco-2 monolayers cultured in DMEM (n = 3) with TEER of 128 ± 11 and 481 ± 23, respectively (Fig. 5). Besides the differences in absolute permeability values in these TEER ranges, also significant changes of permeability patterns could be observed. It should also be emphasized that average values had been gained from different single cultured inserts. The average permeability coefficient of APTS (1.153 µm/min) was at 128 ± 11 Ω cm^2 about 30-fold higher than that (0.0377 µm/min) at 481 ± 23 Ω cm^2. The permeability coefficient of APTS–dextran with 7 glucose units at 128 ± 11 Ω cm^2 was 62.9% as compared to the APTS permeability. This relationship further decreased for APTS–dextran with 14

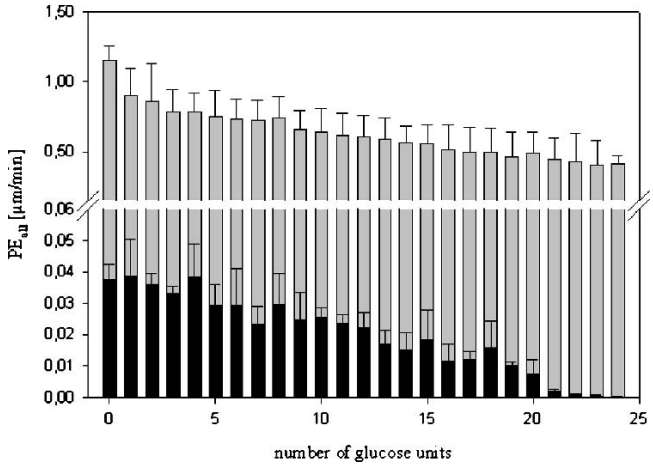

Fig. 5. Size-dependent permeability pattern obtained from transport studies with APTS–dextran 6000 through Caco-2 monolayer (DMEM) at TEER values of 128 ± 11 (gray bars) and 481 ± 23 Ω cm^2 (black bars). Next to obvious differences in absolute PE_{all} values of the single fractions, different slopes of these patterns are recognizable.

Table I. Transport Studies of Diazepam Across Caco-2 Cell Layers Cultured in DMEM and RPMI, ECV304 and PBMEC/C1–2, at Different TEER Values

Cell monolayer	TEER (Ω cm^2)	PE_{all}, diazepam (μm/min)	PE_{cell}, diazepam (μm/min)	Effect of correction
Caco-2 DMEM	445 ± 37	11.03 ± 0.55	16.45 ± 1.20	1.49 ± 0.04
Caco-2 DMEM	245 ± 4	11.42 ± 1.40	17.33 ± 3.21	1.52 ± 0.09
Caco-2 DMEM	128 ± 11	11.21 ± 1.69	16.83 ± 3.83	1.51 ± 0.11
Caco-2 RPMI	118 ± 0	12.33 ± 0.74	19.50 ± 1.89	1.58 ± 0.06
ECV304	122 ± 15	9.65 ± 0.73	13.17 ± 1.38	1.37 ± 0.04
PBMEC/C1–2	100 ± 8	12.24 ± 1.06	18.51 ± 2.43	1.52 ± 0.05

PE_{all} and PE_{cell} of diazepam are presented as mean ± SD (n = 3). Test solutions contained 50 μM diazepam in the appropriate transport medium. Effect of correction (%) means fraction of PE_{cell} values related to PE_{all} values, which is the total permeability through the cell layer, the coating, and finally through the membrane of the insert.

glucose units to 49.1% and finally for APTS–dextran with 21 glucose units to 38.6%. A more significant decline was figured out for permeability coefficients at 481 ± 23 Ω cm^2. Permeability of the APTS–dextran with 7 glucose units was 61.8%, of APTS–dextran with 14 glucose units 39.5%, and of APTS–dextran with 21 glucose units 5.3% related to APTS.

TEER Dependence of Passive, Transcellular Diffusion

To include transcellular pathways in our investigations, transport studies with diazepam were accomplished. In contrast to APTS–dextran, it was sufficient for diazepam detection to transfer the inserts maximum every 60 min. The results of these transport experiments across cell monolayers of Caco-2 cultured in DMEM and RPMI as well as ECV304 and PBMEC/C1–2 at different TEER are summarized in Table I. Diazepam PE_{all} values for all cell lines over a TEER range from 92 to 482 Ω cm^2 were quite similar and ranged from 9.65 ± 0.73 (ECV304) to 12.33 ± 0.74 (Caco-2 in RPMI). Including blank values for PE_{cell} calculation led to an increase of the permeability coefficients. Interestingly, no significant difference of diazepam transport across cell monolayers of Caco-2 cells cultured in DMEM with different TEER (128 ± 11 to 245 ± 4 or to 445 ± 37 Ω cm^2) was observed.

To demonstrate the influence of the coated membrane (PE_{blank}), the effect of correction is assessed. The effect of correction represents the fraction of PE_{cell} divided by PE_{all} and illustrates if the cell monolayer is the main barrier for a distinct transport route. An effect of correction of approximately 1.00 means that the cell monolayer is the major limiting barrier for the transport, and the underlying matrix as well as the filter support have no significant influence on the resulting permeability coefficient. Effect of correction was quite similar for Caco-2 cells cultured in DMEM even in a broad TEER range. Moreover, the results suggest that the membrane of the insert represents a distinct barrier for the diazepam transport. Thus, transport experiments through the coated membrane should be implemented to calculate permeability coefficients (PE_{cell}) specifying the transport through the cell layer only. Compared to diazepam, effects of correction in case of APTS–dextran and Caco-2 cells cultured in DMEM amounted to 1.00 (506 Ω cm^2) or 1.02 (141 Ω cm^2). At 122 Ω cm^2 it increased to 1.10 and finally up to 1.88 at 42 Ω cm^2. Additionally, permeability coefficients PE_{all} of APTS–dextran decreased significantly from 16.32 μm/min at 42 Ω cm^2 to 0.019 μm/min at 506 Ω cm^2. These data confirm that APTS–dextran permeates the cell layer paracellularly. In comparison, PE_{all} values of diazepam were not influenced by increased TEER.

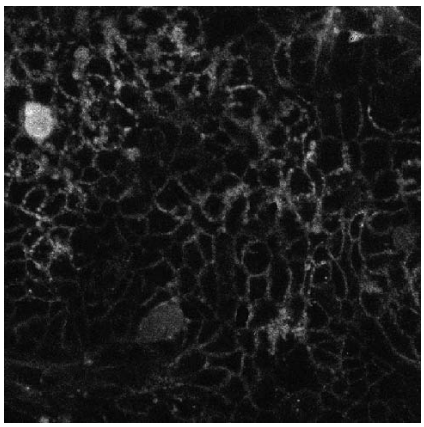

Fig. 6. Confocal laser scanning microscopy image of Caco-2 grown in DMEM after APTS–dextran transport at a TEER of 414 Ω cm^2.

CLSM after Transport Studies with APTS–Dextran

However, to verify the results of previous studies that APTS-labeled dextran is transported paracellularly, Caco-2 cell monolayers were analyzed by CLSM immediately after the transport experiments. As shown in Fig. 6, the observed fluorescence pattern confirms that APTS–dextran cannot penetrate the plasma membrane and is excluded from the cytosol. Thus, APTS–dextran is transported across the Caco-2 monolayer exclusively via the paracellular route.

To collect detailed information about the cellular viability of the examined layer, propidium iodide was added prior to the microscopic inspection. Propidium iodide readily enters cells with injured membranes but is excluded from viable ones characterizing the vitality status of cells. During our investigations, no fluorescence emission >590 nm could be detected indicating that the Caco-2 monolayer is fully viable even after the transport studies.

DISCUSSION

Knowledge about the basal permeability of *in vitro* cell culture models to estimate real changes in permeability is very important (40). To determine the permeability status of cell culture transport models, several markers (mostly radio-

labeled or fluorescent) with distinct molecular size are used. For characterization of the paracellular route they should be hydrophilic, polar, and no substrates for transport systems to exclude contribution of transcellular transport. For smaller molecular weight range, sucrose, mannitol, and fluorescein are often applied; for higher ranges, horseradish peroxidase, albumin, inulin, Evans blue, and dextrans are markers of choice. Additionally, TEER measurement is used to estimate permeability of small ions.

For our studies we have chosen three cell lines. The Caco-2 cell line has been selected because it is a well-established model to study the intestinal transport and exhibits high TEER values. Furthermore, Caco-2 cells are used as a drug permeability model approved by the FDA (10). Thus, the Caco-2 cell line has seemed to be most appropriate as a reference for our BBB cell lines. ECV304 and PBMEC/C1–2 represent BBB models. Doubt has been raised over the use of ECV304 cells for BBB studies and whether these cells are endothelial (41,42). However, several studies have shown that BBB properties were inducible when ECV304 had been cocultured with astrocytes or glioma cell line C6 (19,20,22,23). Furthermore, ECV304 monolayers are able to form tight junctions reflected in higher TEER values, and thus the ECV304 cell line is useful for TEER-dependent studies. In general, tightness studies are of high importance for BBB research. Transport characteristics of the BBB can be altered by diseases as well as by drugs (43–49).

To gain information about paracellular permeability of both small and large molecules, application of a combination of markers (5,6) was indispensable. Therefore, a method was developed that describes cell layer tightness in a size-dependent manner based on similar molecules covering a wide molecular weight range with pharmaceutical relevance. The advantage of our concept using an APTS-labeled dextran ladder for evaluation of paracellular transport is based on structural properties. Each molecule is very hydrophilic carrying three negatively charged sulfonic acid groups. Thus, passive transcellular diffusion is improbable. Moreover, structural characteristics of APTS may hamper binding of APTS–glucose and APTS–maltose to specific active transport systems. Generally, dextran, a glucose polymer, was chosen as marker molecule because it was well established as a marker and represents a suitable molecule for fluorescent labeling due to its easily accessible hydroxyl or carbonyl groups. Following the strategy to label via the carbonyl moiety led to improved analytical properties and complete separation of each single dextran fraction. Additionally, use of radiolabeling and the need for combined application of different markers were avoided.

A commonly used method for determining cell layer tightness is the measurement of the TEER, which represents the paracellular permeability of small ions. To elucidate the correlation between TEER and APTS–dextran permeability, several transport studies were carried out at different TEER values. Madara (50) has reported a nonlinear relationship between electrical resistance and inulin or mannitol permeability. Using fluorescein and FD4 as markers for permeability in an *in vitro* BBB model consisting of bovine brain capillary endothelial cells and astrocytes, Gaillard and de Boer (40) showed an exponential correlation between permeation and TEER. The R^2 value was 0.85 for this exponential decay model for the relationship between the FD4 permeability and the TEER ranging from 22 to 227 Ω cm^2. This exponential correlation could be confirmed with our TEER-dependent experiments with Caco-2 cells cultured in DMEM in the range of 42 to 506 Ω cm^2 with an R^2 value of 0.8958 after linear regression analysis of log PE_{cell} values. Gaillard and de Boer (40) discriminated between P_{app} values for leaky and for tight cell layers and calculated TEER values that demonstrate the limits for the tightness of cell monolayers of their cell model. In this context, they suggested a TEER should be higher than 122 Ω cm^2 for FD4 studies to ensure independence of P_{app} for FD4 from the basal permeability status of their BBB *in vitro* model. This seems to be in concordance with our data. Also, the inflection point (68 Ω cm^2) of the curve depicted in Fig. 3A was in a similar TEER range to the inflection point of the curve of FD4 transport studies of the control experiments published by Gaillard and de Boer (40). It was generally suggested that permeability studies at TEER >150 Ω cm^2 are independent of the basal permeability of the model (40), but the specific limit should be assessed for each *in vitro* model separately. In agreement with these results, it was recommended that endothelial monolayers grown on filters should exhibit a TEER of at least 100 Ω cm^2 or a permeability of less than 1% clearance for FD4 within 2 h to be appropriate for transport experiments (51). However, the permeability status should be proved by the TEER or the permeability of marker molecules before and during transport studies (40).

After transport experiments TEER measurements of both cell monolayers in apical APTS–dextran solutions as well as after supernatant removal and temperature equilibrium in growth media showed no hints of a breakdown of tight junctions. This may indicate that APTS–dextran is not cell toxic and monolayers are fully intact after APTS–dextran application. This was supported by CLSM images, where no fluorescence >590 nm was detected after propidium iodide addition to the cell monolayers prior to the microscopic inspection.

Compared with commonly used FDs, APTS labeling of dextran offers the possibility to distinguish between single fractions. Thus, free APTS, APTS–glucose, and APTS–dextrans with up to 35 glucose units could be determined at once, but still individually, in a single run. Every fraction differs from the neighbored one in the electropherogram by about one glucose unit. This was confirmed by MALDI-MS measurements (52). Therefore, a size-dependent permeability pattern can be provided that is able to reflect the differences in paracellular transport of molecules within a size range relevant for drug transport. In contrast, the application of FDs for transport studies results in the determination of total fluorescence intensities without knowledge of the permeated FD fractions. Consequently, analyzed FD permeability could originate from FITC or small dextrans, whereas, e.g., FITC–dextran 4000 did not pass the monolayer at all. Furthermore, commonly used FDs contain large amounts of nonlabeled molecules, e.g., in FD4 (average MW = 4000 g/mol) statistically 1 dextran of 10 is labeled with FITC. For general tightness determination and detection of significant changes, FDs can mostly be sufficient and in particular well established, because calculation methods for Transwell transport studies correlate the perme-

ated amounts with the stock solution, thus including fluorescent-labeled dextrans only.

However, the APTS–dextran ladder for characterization of cell layer tightness is much more sophisticated. Due to its structural properties and improved CE analytics, it is possible to differentiate between the single fractions of a dextran mixture and thus to determine the real permeabilities. Moreover, it provides information about the paracellular transport of distinct fractions with specified molecular size and thus enables comparison and correlation to other drugs within this specific size range. As described above, the total APTS–dextran permeability decreased at higher TEER. It was hypothesized that bigger molecules should permeate slower than smaller ones when the paracellular transport is restricted and the TEER is increased, respectively. Consequently, the permeability pattern should change dependent on TEER. The data depicted in Fig. 4 proved this hypothesis. The given permeability coefficients were related to the permeability coefficient of APTS and the patterns were displayed for different TEER values. Compared to lower TEER, APTS–dextran with 25 glucose units was not detectable in the given sampling interval at 460 Ω cm^2. Furthermore, the slope of the pattern concurrently decreased with increasing TEER. Figure 5 illustrates the significant changes in permeability patterns at different TEER. Average absolute permeability values of the single fractions were calculated for Caco-2 monolayers cultured in DMEM (n = 3) with TEER of 128 ± 11 and 481 ± 23. Irrespective of the huge differences in the absolute permeability values of single fractions at different TEER, also significant changes in the permeability pattern were observed. Thus, the hypothesis was proved that the slope of permeability pattern decreases with increasing TEER.

The permeability of APTS–dextran illustrates the paracellular transport. To estimate effects of the cell layer tightness on transcellular transport, studies with diazepam at different TEER across Caco-2 cultured in DMEM as well as in RPMI medium and across ECV304 and PBMEC/C1–2 monolayers were performed. This benzodiazepine is known to permeate quite fast into the brain by passive diffusion. Therefore, it is a reliable model substance to characterize transcellular, passive transport across cell monolayers. Results with Caco-2 in DMEM indicated no significant dependence of diazepam permeability on TEER >120 Ω cm^2. In addition to CLSM images (Fig. 6), this proved the paracellular transport of APTS–dextran across the tight junctional barrier, being significantly dependent on TEER. On the other hand, from these results the relevance of highest TEER values for studies of transcellular transport by passive diffusion should be further discussed. Based on these results, it is suggested to include the effect of correction as a parameter to estimate the contribution of the paracellular transport route to the total drug permeability coefficients. Thus, it is postulated that the contribution of the paracellular transport increases with the leakiness of the cell monolayer. At a TEER of about 120 Ω cm^2, the effect of correction was about 1.10 for APTS–dextran transport. Additionally, the asymptotic curve progression of the correlation curve between TEER and APTS–dextran permeability was observed in this TEER range. Moreover, Gaillard and de Boer (40) have reported a similar minimum TEER for transport studies independent of basal permeability. Following on from these results, it is suggested to further investigate if an effect of correction of APTS–dextran 6000 of approximately 1.10 indicates that paracellular transport is negligible with respect to the total permeability coefficient of transcellular transport. According to preliminary results, the effect of correction for APTS–dextran 6000 permeation across different cell layers may differ at the same TEER.

The application of the APTS–dextran ladder is recommended for all permeability determinations to refine detection of changes in paracellular permeability in *in vitro* Transwell as well as in pulsatile, dynamic models. Next to Caco-2, ECV304, and PBMEC/C1–2 cell lines, it also can be useful for cell models like Calu-3 (lung model), RBE4 and BBMEC (blood–brain barrier), choroid plexus cell lines, MDCK, as well as for primary cells in general. The possibility of application for *in vivo* studies with, e.g., rats has to be assessed.

CONCLUSION

The presented technique for characterization of cell layer tightness offers the possibility to generate permeability patterns according to molecular weight. Compared with other currently used methods to evaluate paracellular transport pathways, the APTS–dextran ladder is more precise and enables comparison and correlation to other drugs within a specific molecular weight range. Due to its structural properties and improved CE analytics, it is possible to differentiate between the single fractions of a dextran mixture and thus to determine the real permeabilities to refine, e.g., TEER, FD, sucrose, or Evans blue results. It could be applied for determining the tightness status and the integrity of cell layers, especially for the BBB. Further studies will focus on describing different cell layers to assess whether APTS–dextran permeability patterns are dependent on cell line type at different TEER values. In conclusion, the APTS–dextran ladder is a valuable tool for evaluating the paracellular transport across cell monolayers, being most useful in drug discovery and drug development.

ACKNOWLEDGMENT

We gratefully acknowledge the financial support provided by the Austrian Science Fund FWF (project P–14582 CHE).

REFERENCES

1. W. M. Partridge. *Introduction to the Blood–Brain Barrier*, Cambridge University Press, Cambridge, 1998.
2. I. J. Hidalgo, T. J. Raub, and R. T. Borchardt. Characterization of the human colon carcinoma cell line (Caco-2) as a model system for intestinal epithelial permeability. *Gastroenterology* **96**:736–749 (1989).
3. Y. Liu and C. Anthony Hunt. Studies of intestinal drug transport using an in silico epithelio-mimetic device. *Biosystems* **82**: 154–167 (2005).
4. J. B. Van Bree, A. G. de Boer, M. Danhof, L. A. Ginsel, and D. D. Breimer. Characterization of an "*in vitro*" blood–brain barrier: effects of molecular size and lipophilicity on cerebro-

vascular endothelial transport rates of drugs. *J. Pharmacol. Exp. Ther.* **247**:1233–1239 (1988).
5. M. Boveri, V. Berezowski, A. Price, S. Slupek, A. M. Lenfant, C. Benaud, T. Hartung, R. Cecchelli, P. Prieto, and M. P. Dehouck. Induction of blood–brain barrier properties in cultured brain capillary endothelial cells: comparison between primary glial cells and C6 cell line. *Glia* **51**:187–198 (2005).
6. LK.Hayashi, S. Nakao, R. Nakaoke, S. Nakagawa, N. Kitagawa, and M. Niwa. Effects of hypoxia on endothelial/pericytic co-culture model of the blood–brain barrier. *Regul. Pept.* **123**:77–83 (2004).
7. Y. Ban and L. J. Rizollo. A culture model of development reveals multiple properties of RPE tight junctions. *Mol. Vis.* **3**:18 (1997).
8. P. G. Bannon, M. J. Kim, R. T. Dean, and J. Dawes. Augmentation of vascular endothelial barrier function by heparin and low molecular weight heparin. *Thromb. Haemost.* **73**:706–712 (1995).
9. A. R. Hilgers, R. A. Conradi, and P. S. Burton. Caco-2 cell monolayers as a model for drug transport across the intestinal mucosa. *Pharm. Res.* **7**:902–910 (1990).
10. Center for Drug Evaluation and Research. Food and Drug Administration. Guidance for Industry: Waiver of *in Vivo* Bioavailability and Bioequivalence Studies for Immediate-Release Solid Oral Dosage Forms Based on a Biopharmaceutics Classification System. http://www.fda.gov/cder/guidance/3618fnl.pdf. (accessed 08/15/05).
11. D. A. Volpe, A. B. Ciavarella, E. B. Asafu-Adjaye, C. D. Ellison, P. J. Faustino, and L. X. Yu. Method suitability of a Caco-2 cell model for drug permeability classification. *AAPS Pharm. Sci.* **3**:S1 (2001).
12. D. A. Volpe. Permeability classification of representative fluoroquinolones by a cell culture method. *AAPS Pharm. Sci.* **6**:E13 (2004).
13. G. Wilson, I. F. Hassan, C. J. Dix, I. Williamson, R. Shah, M. Mackay, and P. Artursson. Transport and permeability properties of human Caco-2 cells: an *in vitro* model of the intestinal epithelial cell barrier. *J. Control. Release* **11**:25–40 (1990).
14. F. Delie and W. Rubas. A human colonic cell line sharing similarities with enterocytes as a model to examine oral absorption: advantages and limitations of the Caco-2 model. *Crit. Rev. Ther. Drug Carrier Syst.* **14**:221–286 (1997).
15. F. Joo. Endothelial cells of the brain and other organ systems: some similarities and differences. *Prog. Neurobiol.* **48**:255–273 (1996).
16. A. M. Butt, H. C. Jones, and N. J. Abbott. Electrical resistance across the blood–brain barrier in anaesthetized rats: a developmental study. *J. Physiol.* **429**:47–62 (1990).
17. C. Crone and O. Christensen. Electrical resistance of a capillary endothelium. *J. Gen. Physiol.* **77**:349–371 (1981).
18. K. Takahashi, Y. Sawasaki, J. J. Hata, K. Mukai, and T. Goto. Spontaneous transformation and immortalization of human endothelial cells. *In Vitro Cell. Dev. Biol.* **25**:265–274 (1990).
19. R. D. Hurst and I. B. Fritz. Properties of an immortalized vascular endothelial/glioma cell co-culture model of the blood–brain barrier. *J. Cell. Physiol.* **167**:81–88 (1996).
20. A. S. Easton and N. J. Abbott. Bradykinin increases permeability by calcium and 5-lipoxygenase in ECV304/C6 cell culture model of the blood–brain barrier. *Brain Res.* **953**:157–169 (2002).
21. R. C. Janzer and M. C. Raff. Astrocytes induce blood–brain barrier properties in endothelial cells. *Nature* **325**:253–257 (1987).
22. S. Kuchler-Bopp, J. P. Delaunoy, J. C. Artault, M. Zaepfel, and J. B. Dietrich. Astrocytes induce several blood–brain barrier properties in non-neural endothelial cells. *NeuroReport* **10**:1347–1353 (1999).
23. D. E. M. Dolman, P. Anderson, C. Rollison, and N. J. Abbott. Characterisation of a new *in vitro* model of the blood–brain barrier (BBB). *J. Physiol.* **505**:56–57 (1998).
24. R. Lauer, R. Bauer, B. Linz, F. Pittner, G. A. Peschek, G. Ecker, P. Friedl, and C. R. Noe. Development of an *in vitro* blood–brain barrier model based on immortalized porcine brain microvascular endothelial cells. *Farmaco* **59**:133–137 (2004).
25. M. Teifel and P. Friedl. Establishment of the permanent microvascular endothelial cell line PBMEC/C1–2 from porcine brains. *Exp. Cell Res.* **228**:50–57 (1996).
26. K. Suda, B. Rothen-Rutishauser, M. Günthert, and H. Wunderli-Allenspach. Phenotypic characterization of human umbilical vein endothelial (ECV304) and urinary carcinoma (T24) cells: endothelial *versus* epithelial features. *In Vitro Cell. Dev. Biol. Anim.* **37**:505–514 (2001).
27. G. Vanier, M. Segura, P. Friedl, S. Lacouture, and M. Gottschalk. Invasion of porcine brain microvascular endothelial cells by *Streptococcus suis* serotype 2. *Infect. Immun.* **72**:1441–1449 (2004).
28. G. Vanier, A. Szczotka, P. Friedl, S. Lacouture, M. Jacques, and M. Gottschalk. *Haemophilus parasuis* invades porcine brain microvascular endothelial cells. *Microbiology* **152**:135–142 (2006).
29. P. Benda, J. Lightbody, G. Sato, L. Levine, and W. Sweet. Differential rat glial cell strain in tissue culture. *Science* **161**:370–371 (1968).
30. F.-T. A. Chen and R. A. Evangelista. Analysis of mono- and oligosaccharide isomers derivatized with 9-aminopyrene-1,4,6-trisulfonate by capillary electrophoresis with laser-induced fluorescence. *Anal. Biochem.* **230**:273–280 (1995).
31. A. Guttman, F.-T. A. Chen, R. A. Evangelista, and N. Cooke. High-resolution capillary gel electrophoresis of reducing oligosaccharides labeled with 1-aminopyrene-3,6,8,-trisulfonate. *Anal. Biochem.* **233**:234–242 (1996).
32. F.-T. A. Chen. Characterization of oligosaccharides from starch, dextran, cellulose and glycoproteins by capillary electrophoresis. In P. Thibault S. Honda (eds.), *Methods in Molecular Biology*, Vol. 213, Humana Press Inc., Totowa, NJ, 2003, pp. 105–120.
33. W. Neuhaus, J. Trzeciak, R. Lauer, B. Lachmann, and C. R. Noe. APTS-labeled dextran ladder: a novel tool to characterize cell layer tightness. *J. Pharm. Biomed. Anal.* **40**:1035–1039 (2006).
34. R. M. Arendt, D. J. Greenblatt, D. C. Liebisch, M. D. Luu, and S. M. Paul. Determinants of benzodiazepine brain uptake: lipophilicity *versus* binding affinity. *Psychopharmacology* **93**:72–76 (1987).
35. R. K. Dubey, C. B. McAllister, M. Inoue, and G. R. Wilkinson. Plasma binding and transport of diazepam across the blood–brain barrier. No evidence for *in vivo* enhanced dissociation. *J. Clin. Invest.* **84**:1155–1159 (1989).
36. J. N. Cogburn, M. G. Donovan, and C. S. Schasteen. A model of human small intestinal absorptive cells. 1. Transport barrier. *Pharm. Res.* **8**:210–216 (1991).
37. C. R. Noe, B. Lachmann, S. Mollenbeck, and P. Richter. Determination of reducing sugars in selected beverages by capillary electrophoresis. *Eur. Food Res. Technol.* **208**:148–152 (1999).
38. C. R. Noe, J. Freissmuth, D. Rothley, B. Lachmann, and P. Richter. Capillary zone electrophoresis of carbohydrate mixtures. *Pharmazie* **51**:868–873 (1996).
39. C. R. Noe and J. Freissmuth. Capillary zone electrophoresis of aldose enantiomers: separation after derivatization with *S*-(−)-1-phenylethylamine. *J. Chromatogr., A* **704**:503–512 (1995).
40. P. J. Gaillard and A. G. de Boer. Relationship between permeability status of the blood–brain barrier and *in vitro* permeability coefficient of a drug. *Eur. J. Pharm. Sci.* **12**:95–102 (2000).
41. J. Brown, S. J. Reading, S. Jones, C. J. Fitchett, J. Howl, A. Martin, C. L. Longland, F. Michelangeli, Y. E. Dubrova, and C. A. Brown. Critical evaluation of ECV304 as a human endothelial cell model defined by genetic analysis and functional responses: a comparison with the human bladder cancer derived epithelial cell line T24/83. *Lab. Invest.* **80**:37–45 (2000).
42. H. G. Drexler, H. Quentmeier, W. G. Dirks, and R. A. MacLeod. Bladder carcinoma cell line ECV304 is not a model system for endothelial cells. *In Vitro Cell. Dev. Biol. Anim* **38:** 185–186 (2002).
43. T. Takeda, Y. Yamashita, S. Shimazaki, and Y. Mitsui. Histamine decreases the permeability of an endothelial cell monolayer by stimulating cyclic AMP production through the H2-receptor. *J. Cell. Sci.* **101**:745–750 (1992).
44. N. Borges, F. Shi, I. Azevado, and K. L. Audus. Changes in brain microvessel endothelial cell monolayer permeability induced by adrenergic drugs. *Eur. J. Pharmacol.* **269**:243–248 (1994).
45. S. Fischer, D. Renz, W. Schaper, and G. F. Karliczek. Effects of barbiturates on hypoxic cultures of brain derived microvascular endothelial cells. *Brain Res.* **707**:47–53 (1996).

46. S. Fischer, D. Renz, W. Schaper, and G. F. Karliczek. *In vitro* effects of fentanyl, methohexital, and thiopental on brain endothelial permeability. *Anesthesiology* **82**:451–458 (1995).
47. J. L. Albert, J. P. Boyle, J. A. Roberts, R. A. Challiss, S. E. Gubby, and M. R. Boarder. Regulation of brain capillary endothelial cells by P2Y receptors coupled to Ca^{2+}, phospholipase C and mitogen-activated protein kinase. *Br. J. Pharmacol.* **122**:935–941 (1997).
48. A. G. de Boer and D. D. Breimer. Cytokines and blood–brain barrier permeability. In H. S. Sharma J. Westman (eds.), *Progress in Brain Research*, Elsevier, Amsterdam, 1998, pp. 425–451.
49. R. D. Hurst and J. B. Clark. Alterations in transendothelial electrical resistance by vasoactive agonists and cyclic AMP in a blood–brain barrier model system. *Neurochem. Res.* **23**:149–154 (1998).
50. J. L. Madara. Regulation of the movement of solutes across tight junctions. *Annu. Rev. Physiol.* **60**:143–159 (1998).
51. B. Tewes, H. Franke, S. Hellwig, D. Hoheisel, S. Decker, D. Griesche, T. Tilling, J. and Wegener H. J. Galla. Preparation of endothelial cells in primary cultures obtained from the brains of 6-month-old pigs. In A. G. Boerde W. Sutanto (eds.), *Drug Transport Across the Blood Brain Barrier: in Vitro and in Vivo Techniques*, Harwood Academic Publishers, Amsterdam, 1997, pp. 91–97.
52. H. Suzuki, O. Müller, A. Guttman, and B. L. Karger. Analysis of 1-aminopyrene-3,6,8-trisulfonate-derivatized oligosaccharides by capillary electrophoresis with matrix-assisted laser desorption/ionization time-of-flight mass spectrometry. *Anal. Chem.* **69**:4554–4559 (1997).